

Beware of Pickpockets: A Practical Attack against Blocking Cards

Marco Alecci
SnT, University of Luxembourg
Luxembourg, Luxembourg
marco.alecci@uni.lu

Luca Attanasio
Department of Mathematics,
University of Padova
Padua, Italy
luca_attanasio@me.com

Alessandro Brighente
Department of Mathematics,
University of Padova
Padua, Italy
alessandro.brighente@unipd.it

Mauro Conti
Department of Mathematics,
University of Padova
Padua, Italy
conti@math.unipd.it

Eleonora Losiouk
Department of Mathematics,
University of Padova
Padua, Italy
elosiouk@math.unipd.it

Hideki Ochiai
Department of Electrical and
Computer Engineering, Yokohama
National University
Yokohama, Japan
hideki@ynu.ac.jp

Federico Turrin
Department of Mathematics,
University of Padova
Padua, Italy
turrin@math.unipd.it

Abstract

Today, we rely on contactless smart cards to perform several critical operations (e.g., payments and accessing buildings). Attacking smart cards can have severe consequences, such as losing money or leaking sensitive information. Although the security protections embedded in smart cards have evolved over the years, those with weak security properties are still commonly used. Among the different solutions, blocking cards are affordable devices to protect smart cards. These devices are placed close to the smart cards, generating a noisy jamming signal or shielding them. Whereas vendors claim the reliability of their blocking cards, no previous study has ever focused on evaluating their effectiveness.

In this paper, we shed light on the security threats on smart cards even in the presence of blocking cards, showing the possibility of being bypassed by an attacker. We analyze blocking cards by inspecting their emitted signal and assessing a vulnerability in their internal design. We propose a novel attack that bypasses the jamming signal emitted by a blocking card and reads the content of the smart card. We evaluate the effectiveness of 14 blocking cards when protecting a MIFARE Ultralight smart card and a MIFARE Classic card. We demonstrate that the protection of the 8 blocking cards among the 14 we evaluate can be successfully bypassed to dump the content of the smart card. Based on this observation, we propose a countermeasure that may lead to the design of effective blocking cards. To assist further security improvement, the tool that we developed to inspect the spectrum emitted by blocking cards and set up our attack is made available in open source.

Keywords: Smart Cards, Blocking Cards, Security, RFID

1 Introduction

Today, *smart cards* represent an enabling technology to perform several critical operations like cashless payments, access control, employee IDs, and e-passports. Smart cards are physical cards that embed an Integrated Circuit (IC) chip to store and process data. They can communicate with a reader through physical contact or through short-range wireless protocols. In particular, contactless smart cards rely on the Radio-Frequency IDentification (RFID) standard to interact with a reader without requiring the card to be physically inserted into it. The use of contactless smart cards has been growing in recent years: in 2021, more than 80% of US consumers relied on contactless smart cards, while between 2019 and 2020, there has been a 150% increase in contactless payment transactions [1]. Attackers have widely targeted smart cards [14] through active or passive attacks. The former involves physical access to hardware, leading to probing [35] and reverse engineering [7], while the latter focuses on information leakages, such as power [29] and timing [22] side-channels. Finally, other attacks are executed over the air by relaying [15], eavesdropping [25], and skimming [16]. Attacks against smart cards have a huge impact: According to the Federal Trade Commission, smart card fraud affected 390 million people in the United States in 2021, while identity theft doubled between 2019 and 2020 and has increased in 2021, affecting approximately 1.7 million people [9].

Two alternative approaches can be identified to defend against the above-mentioned attacks: enhancing the inner security of smart cards; introducing an external component to protect them. Considering the former, the ISO/IEC 14443 [19] standard describes the physical characteristics of smart cards available on the market, of which MIFARE is one of the biggest players. According to the specification, there are four types of MIFARE cards, each with an increased security level: (i) the MIFARE Ultralight comes with a 32-bit password, (ii) the MIFARE Classic relies on authentication and encryption methods, being its memory sectors protected by 48-bit keys, (iii) MIFARE Plus uses a 128-bit AES encryption scheme, and (iv) MIFARE DESFire embeds cryptographic algorithms such as symmetric Triple-DES or AES. Although the last two types are used for systems requiring more robust security (e.g., electronic payments, e-passports, identity cards), MIFARE Ultralight and MIFARE Classic are widely used in access control systems, such as public transportation, event ticketing, prepaid applications, loyalty, and amusement [38]. In these scenarios, users can rely on the security introduced by an external component to protect their smart cards, such as blocking cards, blocking wallets, or blocking covers. While covers and wallets generally rely on their metal shielding structure to protect smart cards, blocking cards employ a higher range of approaches (e.g., shielding, jamming), which make themselves more interesting and challenging to be studied from a research point of view.

Blocking cards offer an affordable solution to prevent attacks performed over wireless communications against smart cards. Placed near smart cards, blocking cards protect them through a passive or active approach. On the one hand, passive protection is provided by shielding the communication or emitting a jamming signal based on a received stimulus of specific carrier frequency. On the other hand, active protection involves continuous noise generated without a stimulus. Even though blocking cards are one of the possible countermeasures users can implement, very little information is available from vendors as they wish to keep their internal design secret.

In this work, we perform the first security evaluation of blocking cards. We first analyze their emitted spectrum and identify that most blocking cards emit uncorrelated jamming signals with a Gaussian mixture distribution. We hence demonstrate the vulnerability we found by designing an attack aimed at exfiltrating the content of a smart card when protected by such blocking cards. We assume that the attacker interacts with the victim’s smart card and intercepts the compound signal generated by the blocking card and the smart card by being physically close to the victim. The attacker then elaborates the received signal to remove the noise and extract the content of the smart card. We apply our attack in a proof-of-concept scenario, evaluating the effectiveness of 14 blocking cards in protecting MIFARE Ultralight and MIFARE Classic smart cards. By analyzing their

emitted spectrum, we find that 11 blocking cards are reactive, and the remaining ones shield the smart card. Among the reactive ones, we successfully launch our attack against 8 of them. After identifying the limitations of the current blocking cards’ internal design, we experimentally evaluate the performance of different types of noise to find the ones that really protect smart cards. We believe this study will help vendors strengthen the robustness of their developing blocking cards. Finally, we develop and release a tool that carries out our attack and implements our countermeasure¹.

Our contributions are as follows:

- We perform a security analysis of 14 popular blocking cards at the time of conducting our experiment;
- We design a novel attack aimed at extracting the content of a smart card that is protected by a blocking card. We execute the attack against 14 blocking cards protecting MIFARE cards and evaluate their vulnerability;
- We provide an in-depth analysis of the effectiveness of different types of noise, which may serve as a design guideline for future development of blocking cards;
- We release our tool in open source.

Responsible Disclosure. At the end of our security analysis, in October 2022, we informed the vendors of 6 blocking cards ($\approx 43\%$) about our findings. We could not find contact information for 5 of them (36%), and we chose not to inform the vendors of the 3 blocking cards that we found to have a shielding approach because they successfully protect a smart card. We received a response from 4 out of the 6 we contacted: 2 of them asked not to disclose their brand, and the other 2 did not respond after we shared the vulnerability details. We decided to anonymize all the blocking card brands to have a uniform approach toward them all.

We believe that the reasons for such a low response rate may be two-fold. First, the low price of most blocking cards (i.e., less than \$10 for 13 of them) makes them competitive on the market but discourages their vendors from introducing extra security features. Second, blocking cards come with limited hardware, which might make implementing stronger approaches (e.g., jamming signals or ad-hoc jamming patterns) difficult.

2 Background on Smart cards

In this section, we first provide an overview of smart card technology (i.e., Section 2.1), then we introduce the two smart cards we considered in our scenario: the MIFARE Ultralight (i.e., Section 2.2) and the MIFARE Classic (i.e., Section 2.3).

2.1 Smart Cards Technology

The standard ISO 7816-1 [21] describe smart card with contact technology. This class of cards includes different technologies: magnetic stripe cards, contact smart cards, and

¹<https://github.com/MarcoAlecci/BlockingCardAnalysis>

proximity cards. While contact smart cards must be inserted into the reader to communicate with it, proximity cards rely on the energy transferred by the reader over RFID to power their microprocessor. In fact, proximity cards do not have an internal supply battery and are powered by the reader through electromagnetic (EM) field. In this paper, we focus on proximity cards; whenever we use the “smart card” terminology, we specifically refer to proximity cards.

According to the ISO/IEC 14443 [20] standard, the transmission carrier frequency between the card and the reader is $f_c = 13.56$ MHz, and the reader magnetic field strength is at least $H_{min} = 1.4$ A/m and at most, $H_{max} = 7.5$ A/m. The field strength of the card is approximately 1.5 W/m, resulting in a maximum communication range of 10 cm. The communication between reader and card proceeds as follows: the reader activates the card by applying an EM field; the card waits for a command sent by the reader and when received, might transmit a response; the reader and the card start the communication; the reader deactivates the Radio-Frequency (RF) operating field. Since a reader might already communicate with a card, it relies on the “anti-collision protocol” to select which should receive the message.

2.2 MIFARE Ultralight

The MIFARE Ultralight is the simplest card belonging to the MIFARE family. The first MIFARE Ultralight version had 512 bits (16 pages of 4 bytes) of memory and no security protections. In this paper, we focus on the MIFARE Ultralight EV1 model [31]. This card has a 1024-bit memory, prevents the rewriting of memory pages through One-Time-Programmable bits and a write-lock, and guarantees data access protection through a 32-bit password. It is generally used in different application scenarios that do not involve sensitive data (for example, the cash balance [38]).

2.3 MIFARE Classic

The MIFARE Classic card has more security features than the MIFARE Ultralight. It is based on an NXP Semiconductor proprietary security protocol called CRYPTO-1 for both authentication and encryption of data exchange [32]. Among the different MIFARE Classic cards, we focus on EV1, which is the best in this family. The MIFARE Classic EV1 is available in 1K and 4K memory versions. In both versions, the memory is organized into sectors made up of four or more blocks of 16 bytes each.

In 2008, researchers reverse-engineered the MIFARE Classic chip and recovered the CRYPTO1 algorithm by slicing the chip and taking pictures with a microscope [30]. In the same period, other researchers followed a software-oriented approach and recovered the logical description of the cipher and communication protocol [11, 24]. In particular, in [24] Gans et al. studied the malleability of the CRYPTO1 stream cipher to read all memory blocks of the first sector of the card, while in [11] Garcia et al. reverse-engineered MIFARE

Classic based on the communication behavior between a card and a reader. The result of these previous works is a complete reversal of both the authentication protocol and the encryption algorithm, which led to the identification of several vulnerabilities. The main one is the poor design of the Psuedo-Random Number Generator (PRNG) used by the card to generate the nonce to be sent to the reader, since it is possible to predict the next nonce used by the card [11].

3 Related Work

Since the introduction of Proximity cards for contactless payments in 2007, governments, companies, and researchers have been actively investigating transaction security [14].

Attacks on the Smart Card Hardware. The most common attacks that are effective against smart cards focus on hardware vulnerabilities. These attacks are carried out with techniques including probing [35], reverse engineering [7], or power [29] and timing [22] side-channel analysis. However, these attacks require a skilled attacker and a complicated attacker’s model (e.g., expensive instrumentation and stealing a smart card). Unlike the attacks mentioned above, the attack we propose focuses on the communication between the reader and the card.

Smart Card Communication Attacks. The most well-known communication protocol attack is the relay, first practically introduced by Hancke et al. [15]. This attack aims to transfer the entire communication flow from one payment terminal to another to fraud and charge the victim for a transaction. In [16], the authors show how it is possible to perform a skimming attack on RFID tokens. Another common attack to steal private information stored on the smart card is the snooping attack [23], which consists in accessing unauthorized data from another person or company (e.g., casual observance of the card’s PIN). Other works analyze the authentication protocol of some smart cards, exposing their weaknesses. In [11], the authors successfully attack the authentication protocol of a MIFARE Classic card, while in [12], the authors extend this attack by requiring only wireless access to the card without requiring any RFID reader. In [5], the authors show the feasibility of relay attacks against the EMV payment protocol on smart cards. As we did in this paper, none of the previous works uses a blocking card to protect the smart card.

Jamming. The jamming technique relies on generating radio frequencies to corrupt a wireless communication, either by keeping the medium busy or manipulating the signal received by the receivers. Jammers can rely on different approaches [33]: proactive if the jamming signal is transmitted when data are in the network; reactive if the jamming signal is generated only when there are data in the network; function-specific if the jammer has a specific purpose. Although jamming is usually associated with malicious usage, such a technique has also possible benign applications.

Among those, reactive blocking cards that emit a jamming signal are designed to disrupt the data transmitted by a smart card and prevent an attacker from reading them. Another usage of the jamming technique, which however comes with limitations [18], is the “friendly jamming” or “co-operative jamming” [4, 27], where there is an agreement among the emitter, the receiver, and the jammer so that the jammed signal is still recognizable for the two components involved in the communication, but not for an external eavesdropper. Finally, several anti-jamming techniques [33] have been proposed (e.g., spectrum spreading, frequency hopping). However, previous works [33] stated the ineffectiveness of anti-jamming techniques against RFID systems, which also holds valid for blocking cards we consider in this paper. Thus, our study on the effectiveness of blocking cards is novel and will contribute to enhancing community knowledge.

NFC Communication Defence. Several researchers proposed mechanisms to secure the Near Field Communication (NFC) communication. These defenses are generally designed for smartphone devices because they leverage jamming. In [13], the authors propose *EnGarde*, a hardware-level solution able to protect the smartphone from malicious NFC communication. Similarly, in [40], the authors illustrate a non-invasive hardware solution to protect the smartphone from eavesdropping attacks on NFC communication. More recently, Di Pietro et al. [10] propose a software-level solution to block unwanted NFC communication with the smartphone. Although effective, these solutions are specifically designed for smartphones, restricting the portability of the approach. Instead, the jamming solution we study aims to improve the methods already used in blocking cards, but can also be applied to similar hardware constraint devices.

Blocking Card Analysis. In [39], the video’s presenter evaluated the effectiveness of a blocking card at different distances and positions between the reader and the smart card. The presenter also tried to disassemble it, although he was unsuccessful in his attempt. Our study involves a much more thorough approach since we receive and analyze spectrum of the signal generated by blocking cards based on signal processing techniques. Furthermore, we successfully dissect a shielding card to examine its internal structure.

4 Blocking Cards

This section presents a possible taxonomy to classify blocking cards (i.e., Section 4.1). We then illustrate how we classify our 14 blocking cards by analyzing their emitted power spectrum (i.e., Section 4.2) and their internal physical components (i.e., Section 4.3).

4.1 Blocking Card Taxonomy

Blocking cards provide the most affordable and common defense mechanisms to protect smart cards from over-the-air attacks. However, very little is known about them, not only

because their vendors keep their internal design secret, but also because the academic community has a lack of focus on them. In fact, there is no standard taxonomy for blocking cards in the literature, while we found some vendors and patents that refer to the same types of blocking cards. The first classification criterion for a blocking card is whether it is *passive* or *active*. In particular, passive ones retrieve the energy required for their activation from an external source, whereas active blocking cards come equipped with a battery that allows them to actively emit a jamming signal, which is usually stronger than the passive ones. Due to this choice of internal design, passive blocking cards are cheaper and more diffused than active ones. Furthermore, active blocking cards may even fail to comply with the regulations adopted by some countries due to the unauthorized signal transmission [34]. Passive blocking cards can be distinguished further between *shielding* or *reactive* [3] cards. The former are made of non-conducting materials, such as aluminum foils [36], to block the EM field around the smart card by exploiting the Faraday cage principle (reactive and active cards, instead, disrupt the communication between the smart card and the RF reader). Reactive blocking cards react after a stimulus is received at a given carrier frequency from an NFC reader. Since they are not battery-powered, reactive blocking cards rely on the received RFID energy to power up the jamming signal.

4.2 Classification Based on Spectrum Analysis

We selected the top 14 blocking cards from the Amazon marketplace following its internal recommendation system. Each vendor claims on its website that the card implements RFID protection and, in particular, the NFC communication protection (i.e., operating frequency at 13.56MHz, or HF RFID). Considering our 14 blocking cards, we have no information on their internal design from the vendors, except for one of them being classified as active. Hence, we position each blocking card at about 4cm from an NFC reader and record the emitted signal through a power spectrum analyzer (this distance is empirically identified to prevent saturation issues on the spectrum analyzer side). The recording is carried out with and without the NFC reader activated. In this way, we can discriminate between a continuously emitting active blocking card and a passive one. The analysis of the power spectrum of the signal generated by the blocking card allows inferring its internal design: reactive blocking cards generate noise only when there is an EM field; active blocking cards continuously generate noise, even without a RF field, being battery powered; shielding blocking cards shield the communication, relying on the Faraday principle. Considering our 14 blocking cards, we find that:

- 10 are reactive. This is confirmed by the power level of the spectrum which is low in the absence of a smart card and high in the presence of a smart card.
- 1 is reactive, despite being sold as an active one.

- 3 implement a shielding strategy.

In addition to classifying the blocking cards into passive and active ones, we further inspect their signal to identify the statistical property of the generated noise. To do this, we record the blocking card signal for about 10 seconds. We find that 9 out of the 11 reactive blocking cards produce nearly white Gaussian noise (see Figure 1a), while 2 of the reactive blocking cards produce noise signals at multiple fixed frequencies (see Figure 1b). As an example of white noise, we refer to the power spectrum depicted in Figure 1a, where the power spectral density is approximately constant, except for some peaks at fixed frequencies that include the reader's power. Furthermore, Figure 2a confirms that the distribution can be modeled as a Gaussian mixture. Blocking cards that emit signals at multiple fixed frequencies, as shown in Figure 2b, might have a power spectrum multiplier that creates harmonics as output of its input frequency. Due to space constraints, we reported the power spectrum and Probability Density Function (PDF) in the code repository.

4.3 Classification Based on Physical Inspection

Through the spectrum analysis, we find two blocking cards that do not generate any visible noise. We further analyze them by inspecting their physical properties. As shown in Figure 11a (Appendix A), one of the shielding cards is very flexible, suggesting the absence of a built-in RFID chip to emit jamming signals. After disassembling the card, as shown in Figure 11b (Appendix A), we notice that it has no circuit but a black layer made up of a metallic film that can block the EM field. As a result, this corroborates the idea that these cards leverage shielding materials and the Faraday principle to protect smart cards.

5 System and Threat Model

System Model. In our system model, we assume that the victim uses a smart card for daily activities, such as paying for the public transport used to commute to the workplace or accessing the workplace building. Being aware of the attacks that can be performed against smart cards, the user keeps a blocking card in the wallet to protect his smart card. We further assume that the victim has a smart card belonging to the ISO/IEC 14443 Type A family, which means that it can interact with NFC readers at the 13.56 MHz carrier frequency and a distance of up to 10cm. In particular, the victim has either a MIFARE Ultralight or a MIFARE Classic in his wallet. **Threat Model.** Our attacker aims at extracting the content of the victim's smart card, even though it is accompanied by a blocking card. To achieve this purpose, the attacker has to interact with the victim's smart card and follow a specific communication protocol to dump its content. We assume that the attacker performed some background checks on the victim so that the attacker knows which smart card is

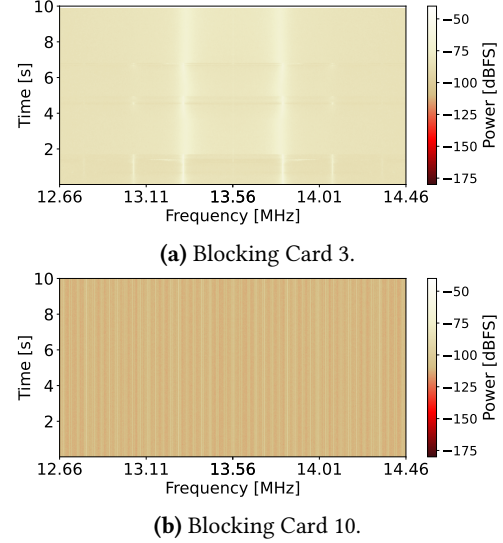


Figure 1. Power spectrum of blocking cards emitting (a) white noise and (b) noise at multiple frequencies.

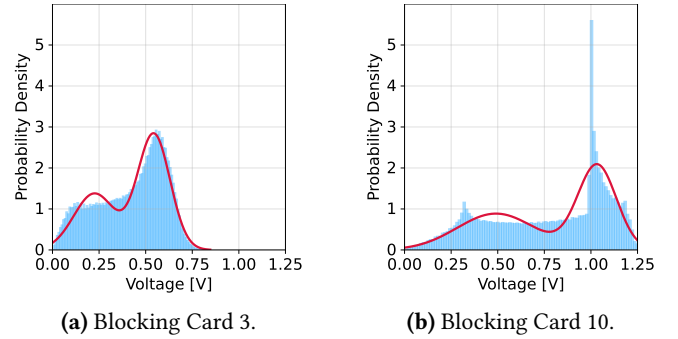


Figure 2. PDF of (a) a blocking card emitting white noise and (b) a card emitting noise at multiple frequencies.

in the wallet. To save the content of the smart card, the attacker first needs an RFID reader configured to send the set of commands compatible with the smart card communication protocol. Since the command set and series of messages for each protocol are publicly available, the attacker can easily get this information. Then, the attacker has to capture the communication between the attacker's own reader and the victim's card, to access the card content, upon removing the noise added by the blocking card through post processing. For signal collection, the attacker can rely on a very cheap setup (less than 50\$): an RF spectrum analyzer connected to an NFC antenna. Alternatively, the attacker might opt for a more expensive solution, which embeds the spectrum analyzer and the antenna in a standalone device. To perform the attack, the attacker has to physically be close to the victim's wallet. Thus, we consider that the attacker can take advantage of a scenario where the victim's wallet is in a static

position (e.g., an office desk or restaurant table). After collecting signals emitted during the communication between the attacker’s reader and the victim’s smart card, the attacker analyzes them to exfiltrate the private information.

6 Proposed Attack

Our attack aims to extract the content of the victim’s smart card, even in the presence of a blocking card. Our attack can be divided into two phases, each depicted in the boxes in Figure 3. The first phase aims at recording the signal emitted by the victim’s smart card and then altered by the blocking card during the communication with the attacker’s reader. The second phase refers to the signal processing performed to remove the noise from the blocking card and extract sensitive information from the smart card. The first phase encompasses only two steps (i.e., receiver activation and message exchange), while the second phase involves four steps (i.e., signal collection, discard of corrupted traces, message reconstruction, and demodulation). In the following, we provide more details of the steps.

Phase I - Step I: Receiver activation. First, we power the RFID receiver to record the card responses.

Phase I - Step II: Messages exchange. The NFC reader, configured by the attacker to communicate with the specific victim’s smart card, starts sending a sequence of messages to the smart card to retrieve its content.

Phase I - Step III: Signal collection. During the communication between the attacker’s NFC reader and the victim’s smart card, the antenna receives the signal generated by the latter. To increase the attack success rate, this step is repeated multiple times to obtain more signal samples.

Phase II - Step I: Discard corrupted traces. Once the signal samples have been collected, the attacker can start processing them. In particular, the attacker first discards all the traces where the noise introduced by the blocking card might generate errors during the upcoming demodulation procedure.

Phase II - Step II: Message Reconstruction. The attacker elaborates the collected signals to reconstruct the original message. In particular, the attacker first extracts portions of the signal where the EM field has been activated. Then, the attacker splits the entire signal into single communication sessions and discriminates the messages belonging to the smart card from the reader’s ones.

Phase II - Step III: Demodulation. After successfully reconstructing the signal, the attacker demodulates it.

7 Attack Implementation

In this section, we first describe the instrumentation we choose for our attack (i.e., Section 7.1) and the implementation details of the general attack components (i.e., Section 7.2). We then illustrate the customization we introduce

to launch the attack against a MIFARE Ultralight (i.e., Section 7.3) and a MIFARE Classic (i.e., Section 7.4).

7.1 Instrumentation

To implement our attack in a real-world scenario, we need two main components: the first is to activate the victim’s smart card and communicate with it; the second is to record the communication signal generated by the smart card and the blocking card, while the communication with the first component is ongoing. We chose an ACR122U reader based on the NXP PN532 module as our first component and an RTL-SDR with a DPL-FANT antenna [26] as the second. The following setup implies that signal processing and demodulation are performed offline after signal acquisition. However, the setup can be easily adapted to a real-time attack.

7.2 General Implementation

Message exchange. To properly configure the ACR122U reader to communicate with the victim’s smart card, we have to write the PN53x chips at the bit level. Thus, we select the libnfc open-source library, which enables the reader to send low-level commands to the smart cards [37]. Since the libnfc library triggers a segmentation fault error when there is the presence of a blocking card, we modified the library to support blocking card collision. The reader sends the same sequence of messages 80 times to allow multiple collection of signals. The time to record 80 communication instances is about 10 seconds.

Signal collection. To collect the communication signal generated by the smart card and the blocking card, we design the GNURadio schema (available in the repository) to control the RTL-SDR. To obtain reliable recordings in the NFC frequency range (i.e., between 0 and 14.4 MHz), we modify the RTL-SDR hardware [2, 28] to enable direct sampling, bypass the tuner, and enable the recording of cleaner signals in the high-frequency range. As a drawback, after this hardware modification, the RF gain is not adjustable, and the RTL-SDR must be at a proper distance from the reader to avoid saturation. As shown in the GNURadio schema, during capture, the signal is filtered by a low-pass filter at a frequency of $f_{\text{cutoff}} = f_c \pm \frac{f_s}{2} = 13.56\text{MHz} \pm 423.75\text{kHz}$. After filtering, we calculate the magnitude of the signal.

Discard corrupted traces. The collected signal is processed through a Python script to remove the noise from the blocking card and retrieve the content of the smart card. To discard the corrupted traces, we verify that the signal values fall below a threshold that we had identified via signal inspection. If the signal values exceed this, then we discard the trace since we cannot process and demodulate it. We also discard a trace if the standard deviation of the signal varies with respect to the standard deviation of the noise, i.e., if $\text{std}(\text{possible_tag}) - \text{std}(\text{noise}) > 0.01$. The rationale underlying this choice is that a slight change in the standard

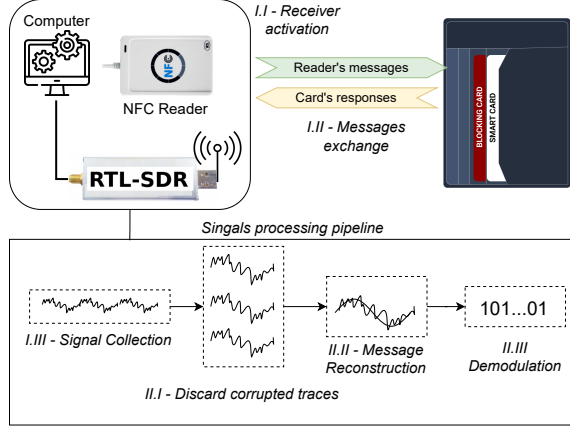


Figure 3. Setup of the attacking steps.

deviation between the possible card signal and the noise allows us to detect the presence of the card signal.

Message Reconstruction. We detect the activation zone of the EM field by applying a moving average technique given the previously defined signal range. Then, we establish message synchronization based on a sliding window algorithm. To detect changes in the signal, and therefore the potential start and end of a message, we calculate the gradient of the signal in each window. Finally, we match each detected message with its sender (reader or card) by using two pre-determined thresholds identified by signal inspection.

Demodulation. After reconstructing the signal, we demodulate it. The demodulator checks if the bits carried in the signal belong to the protocol patterns defined in ISO/IEC 14443 (e.g., Manchester coding modulation). A message sequence generally starts with a start bit, then continues with message bits, and followed by an end bit. The start and end bits of the demodulated sequence are cut, and the bits are inverted according to the ISO/IEC 14443 protocol. The demodulator implementation is available in the repository.

7.3 Customization to Attack the MIFARE Ultralight

The MIFARE Ultralight has no authentication or encryption method. Thus, all communication signals are identical among multiple sessions. Moreover, we assume that this has no password set so that we can read all the card's content. To set up the attack against MIFARE Ultralight, we craft the ACR122U reader to send the set of messages retrieved from the official documentation of MIFARE Ultralight EV1 [31] (for the complete set of messages, refer to Table 2, in Appendix B).

7.4 Customization to Attack the MIFARE Classic

Unlike MIFARE Ultralight, MIFARE Classic comes with enhanced security mechanisms. The communication is encrypted with a per-iteration different nonce; thus, the exact sequence of bytes is different from iteration to iteration. To

perform the entire authentication procedure based on the CRYPTO-1 protocol, we rely on the `crpto1` library used by MIFARE Classic Universal toolKit (MFCUK). MFCUK is an open source C implementation [6] of Dark Side Attack [8]. It uses the libraries `libnfc` and `crpto1` to exploit the weakness of MIFARE Classic CRYPTO1. Similarly to Ultralight, we configure the reader with the Classic sequence of messages, taken from the official MIFARE Classic manual [32]. For the complete set of messages, refer to Table 3, in Appendix C).

8 Attack Evaluation

To evaluate the effectiveness of our attack, we consider 11 blocking cards, among the 14 selected ones, and a MIFARE Ultralight and a MIFARE Classic as smart cards to be protected. We ignore the three that have a shielding approach. In fact, these blocking cards provide effective protection by completely obfuscating the signal from the smart card. We specifically select MIFARE Ultralight and MIFARE Classic smart cards due to their wide adoption in several systems and their lack of internal security mechanisms. We believe that the main use case scenario is to rely on the blocking cards to protect smart cards, which would otherwise be left exposed to attacks. In contrast, smart cards equipped with embedded security mechanisms, such as MIFARE Plus and MIFARE DESFire, make them more challenging to exploit.

Here, we describe our experimental setup (i.e., Section 8.1), our evaluation criteria (i.e., Section 8.2), and the results obtained after demodulating the signals collected from the MIFARE Ultralight (i.e., Section 8.2.1) and from the MIFARE Classic (i.e., Section 8.2.2).

8.1 Setup

Our experimental setup is shown in Figure 4: the reader and antenna are connected to our laptop, while the GNURadio program is running. To simulate a real-world scenario, we assume that the blocking card and the smart card are together in a wallet. The distance between the reader and the wallet is about 3.5cm (this is the maximum distance that allows a reader to interact with a card according to the NFC protocol), and the spacing between two wallet pockets is about 2.5mm.

8.2 Attack Evaluation Criteria

We introduce three metrics to analyze the effectiveness of the 11 blocking cards:

- **Card Detection Rate:** the number of card messages detected by the attacker over the total number of card messages exchanged during the communication.
- **Card Demodulation Rate:** the number of card messages correctly demodulated by the attacker over the total number of card messages exchanged.

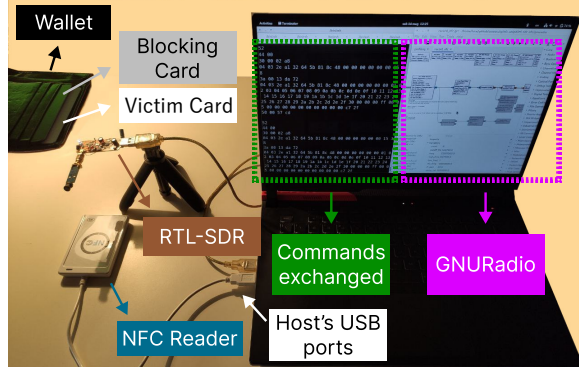


Figure 4. Setup to record the signal of an NFC reader and card in the presence of a blocking card.

- **Attack Success Rate (ASR):** the number of successful attack attempts over the total number of communication repetitions. The attack is considered successful if it can retrieve the content of the smart card.

These measures help us understand whether the card responds to the reader (i.e., the jamming is not effective enough to disrupt the message from the reader to the card) and whether the reader is able to correctly demodulate the response (i.e., the jamming is not effective enough to disrupt the message from the card to the reader). Therefore, thanks to these metrics, it is possible to detect if the card powers up and correctly responds. The three above-mentioned criteria are strongly correlated with each other. In fact, an attack is complete only whether the attacker manages to detect and correctly demodulate the smart card’s messages. In addition, since the attacker’s goal is to read the card content, it is sufficient for the attacker to complete the reading process at least once. Therefore, we consider that a specific blocking card is successfully attacked when $ASR > 0$. We summarize the results achieved with the different blocking cards in Table 1 in Appendix D.

8.2.1 MIFARE Ultralight. In Figure 5a, we report the Card Detection and Demodulation Rates of our attack performed against a MIFARE Ultralight, while Figure 6a shows the ASR. We can see that the attack is successful against 8 blocking cards out of the 11 analyzed, with a varying ASR. Although successful against all blocking cards that generate noise with a Gaussian mixture distribution, our attack shows a varying ASR.

We successfully demodulate smart card messages with a percentage of 100% for Blocking Cards 2 and 7. Instead, our attack does not apply to Blocking Card 6. We conjecture that this has a particular noise distribution that would be robust against our attack. Blocking Cards 9 and 10 produce signals at multiple fixed frequencies, as presented in Section 4.2, and successfully prevent the demodulation of any exchanged

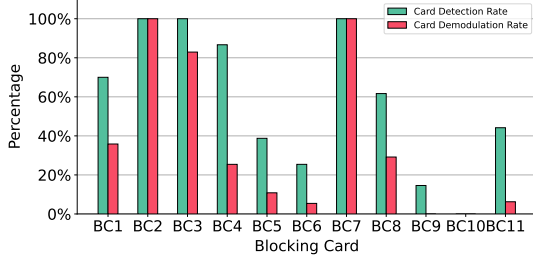
message. Concerning Blocking Card 9, sometimes the communication starts, but one of the subsequent messages is corrupted by noise, thus disrupting the communication session. Furthermore, the RTL-SDR cannot detect any responses from the smart card. Concerning Blocking Card 10, the smart card does not respond in most cases when the reader sends a message. Due to the noise introduced by the blocking cards, the smart card cannot reply or receive a message from the reader.

We recall that we carry out the attack by collecting 80 communications in about 10 seconds. The higher the number of communications collected, the more likely the attack is to be successful. On the other hand, the attacker can achieve a non-negligible chance of success with even less time.

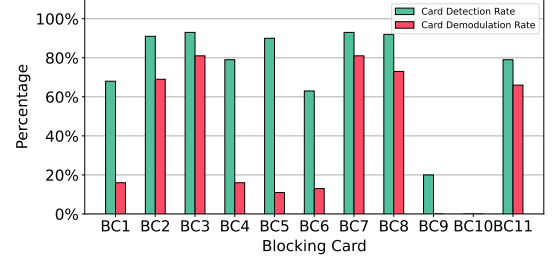
8.2.2 MIFARE Classic. In Figure 5b, we report the Card Demodulation Rate and the Card Detection Rate obtained after executing the attack with the MIFARE Classic smart card. The Card Detection Rate is always above 60% for most of the blocking cards following a white noise approach, which means that MIFARE Classic almost always manages to respond to the reader messages. However, the Card Demodulation Rate drops below 20% with four blocking cards, which means that the demodulator cannot always demodulate the messages sent by the card. In the white noise cases, both the Card Detection Rate and Card Demodulation Rate are high, allowing us to retrieve almost always the entire communication between the card and the reader. The results of Blocking Cards 9 and 10 are similar to the MIFARE Ultralight scenario, since they successfully protect the MIFARE Classic, thus not allowing the card to reply to the messages the reader sends. In fact, none of the card messages is correctly demodulated, and a small number of card messages are detected when analyzing the captured raw signal. This means that Blocking Cards 9 and 10 successfully protect the MIFARE Classic, not allowing the card to reply to the messages sent by the reader.

Figure 6b reports the ASR. We obtain an ASR greater than 80% for five different blocking cards. Unlike the previous case, we can read the smart card when protected by the Blocking Card 6 (i.e., 1 success over the 80 communication).

Overall, in the experiments performed with the MIFARE Classic, we obtain similar results to the scenario with the MIFARE Ultralight. We can complete the attack against the 9 blocking cards out of the 11 evaluated ones. However, to extract the content of a MIFARE Classic, the attacker has to send more messages than the MIFARE Ultralight, thus increasing the probability that the noise added by the blocking card corrupts a message and denies the rest of the communication. Consequently, on average, this reduces the ASR. Once again, the attacker has to find a trade-off between the time spent performing the attack and the success rate.

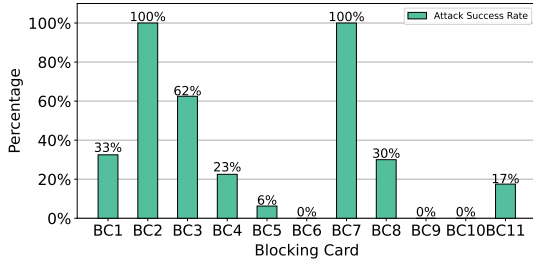


(a) MIFARE Ultralight.

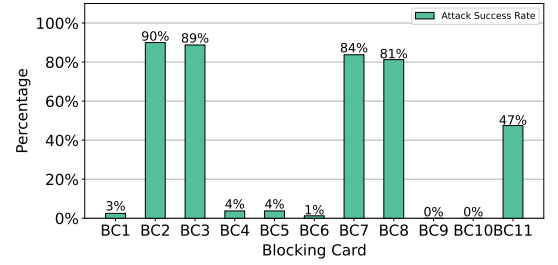


(b) MIFARE Classic.

Figure 5. Card Detection and Demodulation Rates of the attacks on the different cards.



(a) MIFARE Ultralight.



(b) MIFARE Classic.

Figure 6. Attack Success Rate of the attacks on the different cards.

8.3 Demodulation Improvement

To improve the attack performance, we consider reconstructing the original signal with a signal processing technique. In particular, since the noise generated by some of the blocking cards exhibits a close-to-white spectral distribution. The optimal solution for noise removal is signal averaging [17]. Following this procedure, we compute the average of multiple recorded signals and try to reconstruct the original message. However, we only use this technique with the MIFARE Ultralight, since it does not use any random values in the communication. In Figure 7, we report the results using different numbers of averaged signals. As we can notice, by averaging multiple signals, we have a performance improvement in terms of Card Demodulation Rate in some cases. These cases correspond to a blocking card that emits white noise. On the contrary, we have no, or slight, improvement for a blocking card that emits noise at multiple frequencies (i.e., Blocking Cards 9 and 10). We can observe that in all blocking cards, except for Blocking Cards 9 and 10, it is possible to reconstruct the original signal with a single signal. This means that the noise generated by the blocking card, in some cases, is not sufficient to disrupt the original message. This finding motivates the application of the attack with the MIFARE Classic. Indeed, if we can demodulate the original message with non-zero probability with only one signal, it

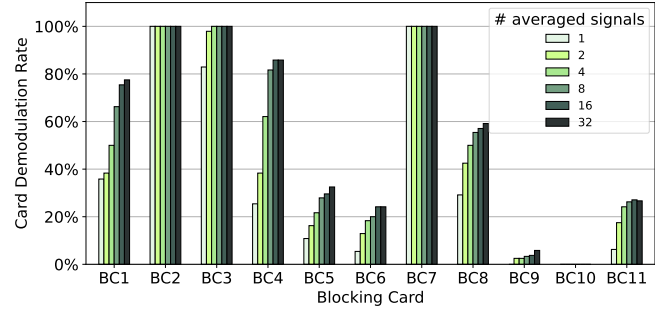


Figure 7. Comparison of Card Demodulation Rate on active and reactive cards by varying the signals averaged. 1 averaged signal indicates a single signal.

is possible to target cards using a freshness mechanism in the authentication phase, i.e., nonces.

9 Countermeasure

As an outcome of our spectrum analysis performed against the 14 blocking cards, we identify three different behaviors adopted to protect a smart card: a shielding approach, which completely obfuscates the signal emitted by the smart card; a noise emitted at multiple fixed frequencies; a noise emitted with a close-to-white spectral distribution. The first two are

successful, as they effectively protect smart cards from malicious attempts to steal their content. In contrast, the third approach allows an adversary to complete an attack like the one we propose in this paper. In this section, we perform an extended analysis of the features that a noise emitted by a blocking card should have to be effective, whether it is a *white* or a *noise emitted at multiple fixed frequencies*. To this purpose, we develop a simulated environment where the noise is directly added to the clean communication signal between the reader and the smart card without considering real-world phenomena such as attenuation or reflection. Then we consider the performance of our demodulator with different noise compositions. We experiment with clear communication recorded with a MIFARE Classic. We measure the performance of the demodulation in terms of the Card Demodulation Rate (introduced in Section 8) and the Reader Demodulation Rate, which can be defined similarly as the number of reader messages correctly demodulated by the attacker over the total number of reader messages exchanged.

White Gaussian noise. In this test, we add white (i.e., uncorrelated) Gaussian noise with different compositions to the clear signal. We first calculate the Standard Deviation (STD) of the original clean signal to estimate its variability. Then, we generate white Gaussian noise signal, using as STD the clean signal STD multiplied by different percentages: 5%, 10%, 15%, 20%, 25%, and 30%. Finally, we sum the original signal with the noisy signal and demodulate the message obtained with the superposition principle. Figure 8 shows an example of the signal obtained.

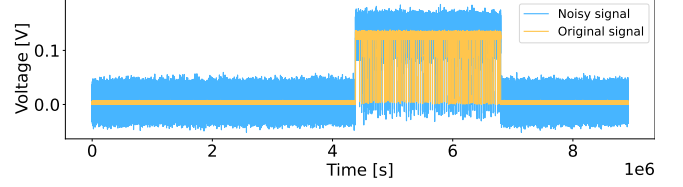


Figure 8. White Gaussian noise 20% added to a clean signal.

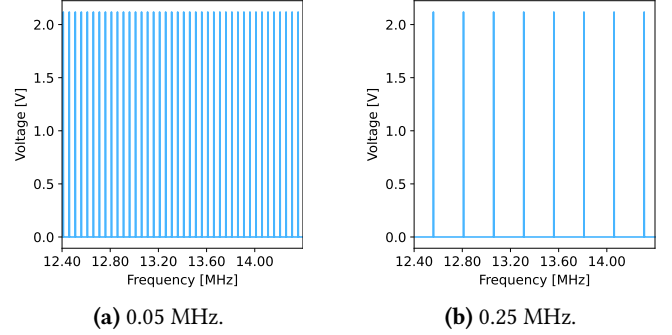


Figure 9. Example of noise at multiple fixed frequencies.

We report the results in Figure 10a. The Card Demodulation Rate significantly decreases when using a white Gaussian noise with a STD greater than a 15% factor, whereas it dramatically drops almost to zero with a factor of 25%. Contrary to this, the reader Demodulation Rate is stable using a low noise factor but decreases significantly using a 30% white Gaussian noise factor.

Noise at multiple fixed frequencies. Here, we use the same setting as the previous analysis to study the effectiveness of adding noise signals at multiple fixed frequencies. More specifically, we generate different noise signals composed of peaks at equally distanced frequencies. As a frequency step (centralized at 13.56 MHz), we experiment: 0.05MHz, 0.10MHz, 0.15MHz, 0.20MHz, 0.25MHz. Figure 9 reports two examples of Fast Fourier Transform (FFT) of the noise added to the clean signal.

We report the results of our demodulation performance in Figure 10b, where we can see the reader Demodulation Rate and the Card Demodulation Rate. We can observe that with a smaller interval distance, i.e., when the FFT plot is very dense, both the Reader Demodulation Rate and the Card Demodulation Rate are very low. They even reach 0% when the distance between two consecutive peaks is only 0.05MHz. On the contrary, when the space is above 0.150MHz, i.e., when the FFT plot is more sparse, both the Reader Demodulation

Rate and the Card Demodulation Rate are rather stable and higher than 70%.

Final considerations on the noise emitted by blocking cards.. Considering the results presented above, we can draw the following conclusions. In the case of *white Gaussian noise*, blocking cards must add a large amount of noise to protect a smart card from malicious attacks. However, reactive blocking cards can only use the RFID energy received from the reader to activate jamming. Therefore, there may be physical limitations in terms of the power of the signal generated. Taking into account the performance of the *noise at multiple fixed frequencies*, we can claim that blocking cards should emit this type of noise with a shallow distance between two consecutive fixed frequencies.

Finally, another strategy that blocking cards can adopt may be to randomly send bits in the transmission frequency bandwidth of the smart card: $13.56\text{MHz} \pm 847.5\text{kHz}$. Similar strategies have been presented in previous works on smartphone NFC communication [10, 13, 40].

10 Conclusion

In this paper, we present the first security analysis on the effectiveness of blocking cards to protect smart cards from attacks carried out over the air. We first propose a methodology to classify blocking cards according to their emitted spectrum. Our procedure allows not only to discriminate between passive and active blocking cards but also to have detailed information about the protection they adopt, which is usually information vendors do not share. We then select 14 popular blocking cards on the market and perform our proposed analysis to identify their internal design. All of

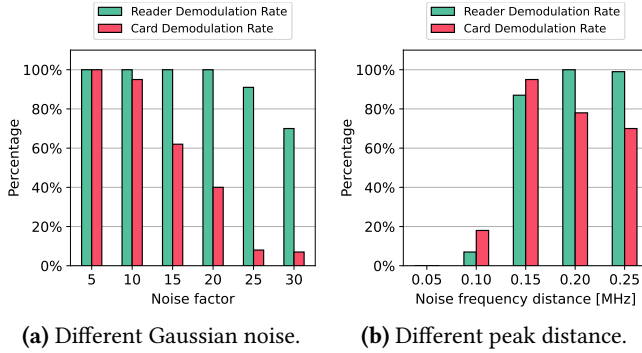


Figure 10. Demodulation results with different noises.

them are passive blocking cards, and, in particular, we find three of them adopting a shielding approach and the remaining others being reactive. To evaluate the effectiveness of such blocking cards, we designed a novel attack aimed at stealing the content of a smart card, even in the presence of a blocking card. Our proposed attack follows a methodology that can be applied to different smart cards operating with the smart card-specific communication protocol at all times. In fact, we select the MIFARE Ultralight and MIFARE Classic smart cards as the target of our attack, and we successfully manage to set it up for both of them without additional adaptations to the communication protocol. We managed to complete our attack with 8 blocking cards out of the 14 selected ones, revealing the limitations of the design of such blocking cards. Finally, we provide an analysis of the statistical properties of emitted noise that are effective in protecting a smart cards, which may serve as a design guideline for further enhancement of blocking cards. Since no previous studies have addressed this topic, we hope that our paper will shed some light on this issue and help improve the security of blocking cards.

References

- [1] 2022. Contactless Payment Statistics in 2022. <https://fitzsmallbusiness.com/contactless-payment-statistics/>.
- [2] Ajoo's Blog. 2017. Intro to RTL-SDR, Part I - Principles and Hardware. <https://web.archive.org/web/20191120002326/http://ajoo.blog/intro-to-rtl-sdr-part-i-principles-and-hardware.html>
- [3] Yves Audebert and Wu Wen. 2006. Blocking contactless personal security device. US Patent App. 11/446,132.
- [4] Daniel S. Berger, Francesco Gringoli, Nicolo Facchi, Ivan Martinovic, and Jens B. Schmitt. 2016. Friendly Jamming on Access Points: Analysis and Real-World Measurements. *Trans. Wireless. Comm.* 15, 9 (2016), 6189–6202.
- [5] Ioana Boureanu and Anda Anda. 2018. Another look at relay and distance-based attacks in contactless payments. *Cryptology ePrint Archive* (2018).
- [6] Andrei Costin. 2022. MFCUK, an open source C implementation of the Courtois Dark Side attack. <https://code.google.com/p/mfcuk/>.
- [7] Franck Courbon, Sergei Skorobogatov, and Christopher Woods. 2016. Reverse engineering flash EEPROM memories using scanning electron microscopy. In *International Conference on Smart Card Research and Advanced Applications*. Springer, 57–72.
- [8] Nicolas T. Courtois. 2009. The Dark Side of Security by Obscurity - and Cloning MiFare Classic Rail and Building Passes, Anywhere, Anytime. *IACR Cryptol. ePrint Arch.* 2009 (2009), 137.
- [9] Lyle Daly and Jack Caporal. 2022. Identity Theft and Credit Card Fraud Statistics for 2022.
- [10] Roberto Di Pietro, Gabriele Oligeri, Xavier Salleras, and Matteo Signorini. 2018. N-Guard: a Solution to Secure Access to NFC tags. In *2018 IEEE Conference on Communications and Network Security (CNS)*. IEEE, 1–9.
- [11] Flavio D Garcia, Gerhard de Koning Gans, Ruben Muijers, Peter van Rossum, Roel Verdult, Ronny Wichers Schreur, and Bart Jacobs. 2008. Dismantling MIFARE classic. In *European symposium on research in computer security (ESORICS)*. Springer, 97–114.
- [12] Flavio D. Garcia, Peter van Rossum, Roel Verdult, and Ronny Wichers Schreur. 2009. Wirelessly Pickpocketing a Mifare Classic Card. In *2009 30th IEEE Symposium on Security and Privacy (S&P)*. 3–15.
- [13] Jeremy J. Gummesson, Bodhi Priyantha, Deepak Ganesan, Derek Thrasher, and Pengyu Zhang. 2013. EnGarde: Protecting the Mobile Phone from Malicious NFC Interactions. In *11th Annual International Conference on Mobile Systems, Applications, and Services*. 445–458.
- [14] BB Gupta and Megha Quamara. 2021. A taxonomy of various attacks on smart card-based applications and countermeasures. *Concurrency and Computation: Practice and Experience* 33, 7 (2021), 1–1.
- [15] Gerhard P Hancke. 2005. A practical relay attack on ISO 14443 proximity cards. *Technical report, University of Cambridge Computer Laboratory* 59 (2005), 382–385.
- [16] Gerhard P Hancke. 2011. Practical eavesdropping and skimming attacks on high-frequency RFID tokens. *Journal of Computer Security* 19, 2 (2011), 259–288.
- [17] Umer Hassan and Muhammad Sabieh Anwar. 2010. Reducing noise by repetition: introduction to signal averaging. *European Journal of Physics* 31, 3 (2010), 453.
- [18] Qiao Hu, Lavinia Mihaela Dinca, Anjia Yang, and Gerhard Hancke. 2016. Practical limitation of co-operative RFID jamming methods in environments without accurate signal synchronization. *Computer Networks* 105 (2016), 224–236.
- [19] ISO/IEC 14443-1:2018 2018. *Cards and security devices for personal identification — Contactless proximity objects — Part 1: Physical characteristics*. Technical Report.
- [20] ISO/IEC 14443-2:2020 2020. *Cards and security devices for personal identification — Contactless proximity objects — Part 2: Radio frequency power and signal interface*. Technical Report.
- [21] ISO/IEC 7816-1:2011 2011. *Identification cards — Integrated circuit cards — Part 1: Cards with contacts — Physical characteristics*. Technical Report.
- [22] Paul C Kocher. 1996. Timing attacks on implementations of Diffie-Hellman, RSA, DSS, and other systems. In *Annual International Cryptology Conference*. Springer, 104–113.
- [23] Divyan M Konidala, Zeen Kim, and Kwangjo Kim. 2007. A simple and cost-effective RFID tag-reader mutual authentication scheme. In *International Conference on RFID Security (RFIDSec)*. 141–152.
- [24] Gerhard de Koning Gans, Jaap-Henk Hoepman, and Flavio D Garcia. 2008. A practical attack on the MIFARE Classic. In *International Conference on Smart Card Research and Advanced Applications*. Springer, 267–282.
- [25] Henning Kortvedt and S Mjolsnes. 2009. Eavesdropping near field communication. In *The Norwegian Information Security Conference (NISK)*, Vol. 27. 5768.
- [26] Frédéric Le Roy, Thierry Quiniou, Ali Mansour, Raafat Lababidi, and Denis Le Jeune. 2016. RFID Eavesdropping Using SDR Platforms. In *International Conference on Applications in Electronics Pervading Industry, Environment and Society*. Springer, 208–214.

- [27] Xuran Li, Hong-Ning Dai, and Hao Wang. 2016. Friendly-Jamming: An Anti-Eavesdropping Scheme in Wireless Networks of Things. In *IEEE Global Communications Conference (GLOBECOM)*. 1–6.
- [28] livedoor. 2012. RTL-SDR hardware modification for receiving HF signals. <http://blog.livedoor.jp/bh5ea20tb/archives/4263275.html>
- [29] Stefan Mangard, Elisabeth Oswald, and Thomas Popp. 2008. *Power analysis attacks: Revealing the secrets of smart cards*. Vol. 31.
- [30] Karsten Nohl, David Evans, Starbug, and Henryk Plötz. 2008. Reverse-Engineering a Cryptographic RFID Tag. In *USENIX Security Symposium*.
- [31] NXP Semiconductors. 2014. MIFARE Ultralight EV1 - Contactless ticket IC Datasheet - Rev. 3.3. <https://www.nxp.com/docs/en/data-sheet/MF0ULX1.pdf>
- [32] NXP Semiconductors. 2017. MIFARE Classic EV1 4K - Mainstream contactless smart card IC for fast and easy solution development - Rev. 3.2. https://www.nxp.com/docs/en/data-sheet/MF1S70YYX_V1.pdf.
- [33] Hossein Pirayesh and Huacheng Zeng. 2022. Jamming Attacks and Anti-Jamming Strategies in Wireless Networks: A Comprehensive Survey. *IEEE Communications Surveys & Tutorials* 24, 2 (2022), 767–809.
- [34] RFID4u. 2022. RFID Basics - RFID Regulations. <https://rfid4u.com/rfid-regulations/>.
- [35] Qihang Shi, Domenic Forte, and Mark M Tehranipoor. 2017. Analyzing circuit layout to probing attack. In *Hardware IP Security and Trust*. 73–98.
- [36] Yakov Pytor Shkolnikov, Yanqing Du, and Brad Alexander McGoran. 2011. Shield for radio frequency ID tag or contactless smart card. US Patent 7,936,274.
- [37] Roel Verdult and Francois Kooman. 2011. Practical Attacks on NFC Enabled Cell Phones. In *2011 Third International Workshop on Near Field Communication*. 77–82.
- [38] Wikipedia. 2022. MIFARE - Places that use MIFARE products. <https://en.wikipedia.org/wiki/MIFARE>.
- [39] Zerobrain. 2019. Test! RFID / NFC Blocker Karten - Schutz oder Placebo? <https://www.youtube.com/watch?v=2G14xtHcAYY>
- [40] Ruogu Zhou and Guoliang Xing. 2014. nshield: A noninvasive nfc security system for mobile devices. In *Proceedings of the 12th annual international conference on Mobile systems, applications, and services*. 95–108.

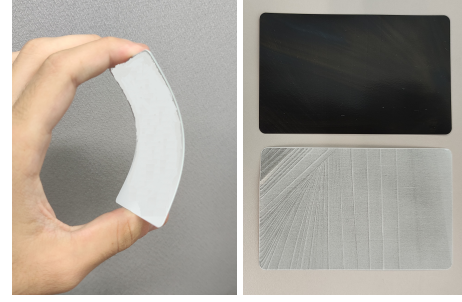
Appendix

A Shielding Card Dissection

In Figure 11 we report an image showing the physical composition of a shielding blocking card that highlight the absence of an integrated circuit.

B MIFARE Ultralight Message Set

Table 2 reports the list of messages exchanged between the reader and the MIFARE Ultralight during the signal acquisition [31].



(a) Shielding card flexibility. (b) Shielding card internal.

Figure 11. Physical characteristics of a shielding blocking card.

Table 2. Messages that were repeatedly exchanged (80 times) between the reader (R) and the card (C).

Device	Command	Arg1	Arg2
R	WUPA		
C	ATQA		
R	READ from page 00h	00 (Addr)	
C	result of READ		
R	FAST READ	00h (StartAddr)	13 (EndAddr)
C	FAST READ result		
R	HALT		

C MIFARE Classic Message Set

Table 3 reports the list of messages exchanged between the reader and the MIFARE Classic during the signal acquisition.

Table 3. Set of messages exchanged between the reader (R) and the MIFARE Classic (C).

Step	Device	Command
1	R	WUPA
2	C	REQA
3	R	SELECT
4	C	UID + BCC
5	R	SELECT + UID
6	C	MIFARE 1K
7	R	AUTH (Block 0x07)
8	C	n_T
9	R	$n_R \oplus ks_1 + a_R \oplus ks_2$
10	C	$a_T \oplus ks_3$
11	R	READ
12	C	Result of READ
13	R	HALT

D Summary of Results

In Table 1 we summarize the results achieved with the different blocking cards.

Table 1. Summary of the results on the various Blocking Cards.

Blocking Card ID	Type	MIFARE Ultralight			MIFARE Classic			MIFARE Ultralight Demodulation Improvment					
		Detection Rate	Demodulation Rate	ASR	Detection Rate	Demodulation Rate	ASR	1	2	4	8	16	32
1	Gaussian	0.70	0.36	0.33	0.68	0.16	0.03	0.38	0.38	0.50	0.66	0.75	0.78
2	Gaussian	1.00	1.00	1.00	0.91	0.69	0.90	1.00	1.00	1.00	1.00	1.00	1.00
3	Gaussian	1.00	0.83	0.63	0.93	0.81	0.89	0.83	0.98	1.00	1.00	1.00	1.00
4	Gaussian	0.87	0.25	0.23	0.79	0.16	0.04	0.25	0.38	0.62	0.82	0.86	0.86
5	Gaussian	0.39	0.11	0.06	0.90	0.11	0.04	0.11	0.16	0.22	0.28	0.30	0.33
6	Gaussian	0.25	0.05	0.00	0.63	0.13	0.01	0.05	0.13	0.18	0.20	0.24	0.24
7	Gaussian	1.00	1.00	1.00	0.93	0.81	0.84	1.00	1.00	1.00	1.00	1.00	1.00
8	Gaussian	0.62	0.29	0.30	0.92	0.73	0.81	0.29	0.43	0.50	0.55	0.57	0.59
9	Fixed frequencies	0.01	0.00	0.00	0.20	0.00	0.00	0.00	0.03	0.03	0.03	0.04	0.06
10	Fixed frequencies	0.00	0.00	0.00	0.00	0.00	0.00	0.00	0.00	0.00	0.00	0.00	0.00
11	Gaussian	0.44	0.06	0.18	0.79	0.66	0.48	0.06	0.18	0.24	0.26	0.27	0.27
12	Shielding	-	-	-	-	-	-	-	-	-	-	-	-
13	Shielding	-	-	-	-	-	-	-	-	-	-	-	-
14	Shielding	-	-	-	-	-	-	-	-	-	-	-	-